

Dynamics of volcanic and meteorological clouds produced on 26 December (Boxing Day) 1997 at Soufrière Hills Volcano, Montserrat

G. C. MAYBERRY, W. I. ROSE & G. J. S. BLUTH

Department of Geological Engineering and Sciences, Michigan Technological University, Houghton, MI 49931, USA

Abstract: The 26 December 1997 explosive activity of Soufrière Hills Volcano, Montserrat, provided an opportunity to study the evolution of a volcanic cloud by merging data from various satellites with wind-trajectory data. The activity involved a debris avalanche that descended SSW from the lava dome, to the coast, and a pyroclastic density current that traversed the coast and entered the sea. The slope failure and subsequent dome collapse occurred at *c.* 07:01 universal time (UT; 03:01 local time), lasted 15.2 minutes, and produced an upwardly convecting volcanic ash cloud that cloud temperatures suggest rose to *c.* 15 km. The volcanic ash cloud was unusual because the pyroclastic density current transported hot fine ash to the sea, where it rapidly transferred its heat to the sea water. The evaporation of large volumes of water produced a volcanogenic meteorological (VM) cloud that convected along with the volcanic ash cloud.

The evolution of the volcanic and VM clouds was studied using an isentropic wind trajectory model and data from three satellite sensors: Geostationary Observational Environmental Satellite 8 (GOES 8), Advanced Very High Resolution Radiometer (AVHRR), and Total Ozone Mapping Spectrometer (TOMS). The high temporal resolution of the GOES 8 images filled many of the time gaps the other satellites left, and allowed quantitative retrievals to be performed using a two-band infrared retrieval method. The three-dimensional morphology of the volcanic cloud was reconstructed using GOES 8 data and by determining the heights of air parcels from wind-trajectory data. The volcanic cloud was estimated to contain up to 4.5×10^7 kg of silicate ash. Between *c.* 07:39 UT and 13:39 UT the ash signal of the volcanic cloud was masked by the VM cloud, which had a mass of up to 1.5×10^8 kg of ice. Ice forms when moist air is convected upwards to temperatures of less than -40°C and becomes saturated.

Ice formation in volcanic clouds is especially likely when hot volcanic material is cooled by seawater rather than the atmosphere. The efficiency of evaporation of the seawater was calculated to be *c.* 5%, based on physical and GOES 8 data. TOMS data showed the SO_2 in the volcanic cloud rose higher than the ash in the volcanic cloud, as has occurred in several other eruptions.

A comparison between GOES 8 and AVHRR data showed that AVHRR data retrieved higher fine-ash silicate masses and higher cloud areas than GOES 8 due to the finer spatial resolution of AVHRR images. The effect on retrieval data of the high water vapour content in the lower troposphere of the tropical atmosphere was quantified; the high humidity in the Montserrat region caused the characteristic ash signal to the infrared sensors to be depressed by up to 80%. This signal depression caused a corresponding underestimation of the mass and area of the volcanic cloud when the infrared brightness temperature difference retrieval technique was used.

Over the last two decades scientists have pursued progressively more sophisticated methods of using satellite data for the study of volcanic clouds (e.g. Krueger 1983; Prata 1989; Wen & Rose 1994; Krotkov *et al.* 1999). Most recently, the merging of satellite and wind-trajectory data has provided a more holistic look at volcanic cloud behavior. Studies of the 1994 Rabaul eruption demonstrated that the eruption cloud contained large amounts of ice (Rose *et al.* 1995). Data showed that the June 1992 Spurr eruption cloud was sheared and thinned from below as it travelled away from the volcano (Shannon 1996). The 1982 El Chichón eruption cloud was found to have separated into SO_2 and ash-rich portions at different altitudes (Schneider *et al.* 1999). In addition, the high temporal resolution of geostationary infrared data has provided an opportunity to perform more detailed analysis of volcanic clouds by filling in the time gaps left by polar orbiting satellites (Rose & Schneider 1996). The development of quantitative algorithms for retrieving the characteristics of volcanic clouds has made it possible to evaluate reactions and chemical/physical processes in volcanic clouds as they move (Wen & Rose 1994; Krueger *et al.* 1995; Krotkov *et al.* 1999).

While preliminary work has been conducted on the use of geostationary satellites in quantitative volcanic cloud studies (Rose & Schneider 1996; Davies & Rose 1998), a need exists for multisensor studies to ensure that the high temporal resolution of geostationary satellite data and the high spatial resolution of polar orbiting satellite images are used to their full potential. Over 800 scenes of volcanic clouds from Soufrière Hills Volcano are available for analysis (Davies & Rose 1998). Davies & Rose (1998) briefly describe some details of the evolution of the volcanic cloud from the 6 November 1997 dome collapse of Soufrière Hills Volcano. They discuss the presence of a volcanogenic meteorological (VM) cloud, and the effect of using the brightness temperature difference (BTD) technique to delineate the volcanic cloud in a region with high humidity.

Several volcanic cloud studies using polar-orbiting satellites have shown that separation of SO_2 from the ash in volcanic clouds occurred (Shocker 1996; Schneider *et al.* 1999; Constantine *et al.* 2000), but the cause of the separation has not been explained. The

frequent data provided by geostationary satellites are needed to study the physical and chemical processes in short-lived volcanic clouds.

The goal of this paper is to describe and analyse the dynamics of volcanic and VM clouds utilizing satellite and wind-trajectory data. This work applies diverse satellite and wind-trajectory model methodology to the largest Soufrière Hills eruptive event of 1997, the 26 December dome collapse, which generated a pyroclastic density current that travelled to the coast and entered the sea, producing a VM cloud from evaporation of seawater and a volcanic cloud that rose to *c.* 15 km. To help describe and analyse the clouds, data from Geostationary Observational Environmental Satellite 8 (GOES 8), the Advanced Very High Resolution Radiometer (AVHRR), the Total Ozone Mapping Spectrometer (TOMS), an isentropic wind trajectory model, and ground observations are used.

The main objectives of this study are as follows. (a) Determine the three-dimensional morphology of the volcanic cloud using wind-trajectory data and GOES 8 imagery. (b) Compare the imagery and ash cloud retrieval data from AVHRR and GOES 8 which have different spatial resolutions. (c) Analyse the masking effect of the VM cloud when it overlapped the volcanic cloud from the satellite perspective. The evolution of the VM cloud is reconstructed, the volume of seawater evaporated to form it is estimated, and the effect of masking by the VM cloud on retrieved volcanic-cloud data is discussed. (d) Investigate the effect of the humid lower troposphere in the Montserrat region on retrieving cloud properties using the infrared brightness temperature difference technique. (e) Investigate the cause of the separation of SO_2 and volcanic ash in the Soufrière Hills volcanic cloud.

The 26 December 1997 collapse

The largest dome collapse of the Soufrière Hills eruption occurred on 26 December 1997. The SW flank gave way and moved down the White River valley as a debris avalanche (Sparks *et al.* 2002). This

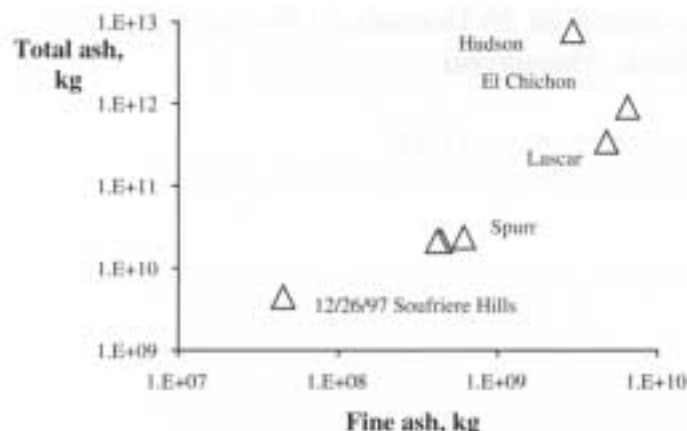


Fig. 1. Ash masses in volcanic clouds. The total mass of ash in measured and mapped fallout deposits is plotted against the maximum mass of fine (diameter 1–25 μm) ash measured in volcanic clouds using two-band infrared satellite data (Rose *et al.* 2000).

was followed by a fast-moving pyroclastic density current which generated an important volcanic cloud (Bonadonna *et al.* 2002). While the 26 December 1997 volcanic ash cloud is large relative to other Soufrière Hills volcanic clouds, it is an order of magnitude smaller than those of 1992 from Crater Peak of Mount Spurr, Alaska, and more than two orders of magnitude smaller than the 15 August 1991 eruption of Cerro Hudson, Chile (Fig. 1). Details of the 26 December 1997 event are given by Sparks *et al.* (2002). As the pyroclastic density current travelled down White River Valley to the sea, it quickly overtook the debris avalanche. Sparks *et al.* (2002) used estimates of the volume of the dome before and after the eruption to estimate the volume of dome material in the pyroclastic density current at $35\text{--}45 \times 10^6 \text{ m}^3$ (c. 40% of the dome). The density current had a peak velocity of $80\text{--}90 \text{ m s}^{-1}$, and a minimum flux of 10^6 kg s^{-1} . It devastated 10 km^2 of southern Montserrat and extended the former coastline a distance of up to 200 m. The dispersal of the material from the pyroclastic density current is described by Sparks *et al.* (2002) and Ritchie *et al.* (2002). The fine ash (0.05–63.5 μm radius; Baxter *et al.* 1999) component of the pyroclastic density current convected, due to thermal differences between air heated by the hot ash and ambient air, forming a column that rose several kilometres into the atmosphere (Cole *et al.* 1998). Light ash fell over southwestern Montserrat, as well as SE of Montserrat on the island of Guadeloupe, but most of the fine ash was deposited in the sea (Bonadonna *et al.* 2002). Approximately $1.8\text{--}3.2 \times 10^6 \text{ m}^3$ of the $35\text{--}45 \times 10^6 \text{ m}^3$ of dome material was deposited on land, therefore about $30\text{--}43 \times 10^6 \text{ m}^3$ of the material is not accounted for (Sparks *et al.* 2002). This missing volume is thought to have partly entered the sea, and partly convected into the buoyant ash plume. Though the lateral extent of the submarine deposit is unknown, areas with deposits up to 50 m thick were found, suggesting that the bulk of the missing material was deposited in the sea (Sparks *et al.* 2002).

The activity occurred at night and could not be observed directly, so we know little about the interaction between the pyroclastic density current and the ocean. However, it is probable that the entry of the pyroclastic density current into the sea caused evaporation of seawater and the formation of a VM cloud.

Fallout deposits of 26 December 1997

Only a small fraction of the airborne ash of 26 December 1997 was sensed by infrared satellite detectors because much of it was coarser than the satellite could detect (1.5–12 μm radius) and fell out very quickly after the eruption. Andesitic ash produced by fragmentation of the Montserrat lava dome during various dome collapses contained 60–70 wt% of 5–62.5 μm particles and 13–20 wt% par-

ticles <5 μm (Baxter *et al.* 1999). Although the ash was fine-grained and would be expected to have a long atmospheric residence, much of it fell out very quickly as accretionary lapilli SW of the volcano (Bonadonna *et al.* 2002). The high humidity in the tropical atmosphere, and/or the excess water in the volcanic cloud from interaction with the VM cloud, may have been factors in the creation of the large quantity of accretionary lapilli.

Meteorology of the Montserrat region

The weather in the Caribbean is often monotonous, with patterns that can last for weeks. Conditions near sea level are hot and dry, and mountains are often draped with orographic clouds. Beneath the temperature inversion (1–2 km), the air is moist with a layer of cumulus clouds. The trade winds, or tropical easterlies, are pronounced in the tropics between 0 and 6 km, especially during the winter. The trade winds produce predictable weather patterns because they travel consistently towards the SW at c. 7 m s^{-1} , while upper level winds (>6 km) often travel in a different direction (Barry & Chorley 1992). The tropopause in late December, based on radiosonde data from Guadeloupe, was about 16–17 km above sea level.

Data and data analysis

Geostationary Observational Environmental Satellite (GOES)

GOES sensors utilize five bands ranging from visible to thermal-infrared (Table 1) and operate at the geosynchronous altitude of 35 800 km above the Earth's surface. Geostationary data are advantageous when studying volcanic clouds because the data have a fine temporal resolution. Images are collected approximately every 30 minutes compared to two to four times daily for polar-orbiting satellites. The 26 December 1997 activity was imaged by

Table 1. GOES 8 and AVHRR spectral band information

Band	GOES λ (m)	Resolution (km)	AVHRR λ (m)
1	0.55–0.75	1	0.58–0.68
2	3.8–4.0	4	0.725–1.10
3	6.5–7.0	8	3.55–3.93
4	10.2–11.2	4	10.3–11.3
5	11.5–12.5	4	11.5–12.5

* AVHRR subpoint resolution is 1.1 km in all bands.

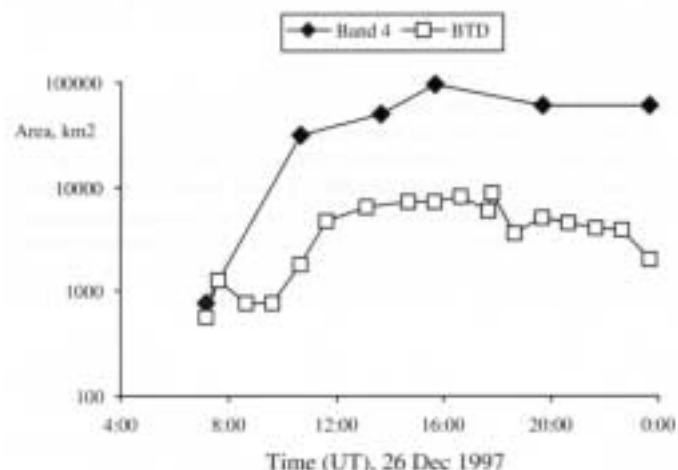


Fig. 2. Area of the volcanic cloud of Soufrière Hills Volcano, 26 December 1997, as determined by GOES band 4 and BTD. The BTD area matches the band 4 area only early in the event and generally is about 10% of the band 4 area, decreasing with time.

GOES 8 which scans bidirectionally, alternating west to east and east to west (Kidder & Vonder Haar 1995).

Advanced Very High Resolution Radiometer (AVHRR)

The AVHRR is a multispectral, infrared radiometer that operates on polar-orbiting meteorological satellites operated by the National Oceanic and Atmospheric Administration (NOAA) with five spectral bands (Table 1). The 26 December 1997 volcanic cloud was imaged by the AVHRR sensor on NOAA-14, which is a sun-synchronous satellite, with a daytime north-to-south equatorial crossing (Lillesand & Kiefer 1987). AVHRR has a swath width of approximately 2800 km, and images the same area twice daily with daytime and night-time passes. Local area coverage (LAC) data (pixel scale 1.1 km at nadir) were used in this study to analyse physical details of the volcanic cloud.

Retrieval methods for GOES and AVHRR

In order to discriminate the volcanic cloud from the background and from meteorological clouds, the brightness temperature difference (BTD) between bands 4 and 5 was used (Prata 1989). The effective radius and optical depth of the volcanic cloud at infrared wavelengths was then retrieved using a radiative transfer model developed by Wen & Rose (1994). The model has simplifying case-dependent assumptions. The cloud is assumed to be $c. 1$ km thick, homogeneous, semi-transparent, parallel to the surface below it, and the atmosphere above and below the cloud is assumed to be cloud-free. It is also assumed that particles in the cloud are all andesitic, spherical in shape with a log-normal size distribution. The scheme detects those particles with radii of $1.5\text{--}12\ \mu\text{m}$, sizes that experience Mie scattering and absorption at infrared wavelengths (Wen & Rose 1994). Band 4 ($10.2\text{--}11.2\ \mu\text{m}$) of the GOES 8 sensor is slightly offset from band 4 ($10.3\text{--}11.3\ \mu\text{m}$) of the AVHRR sensor (Table 1), and

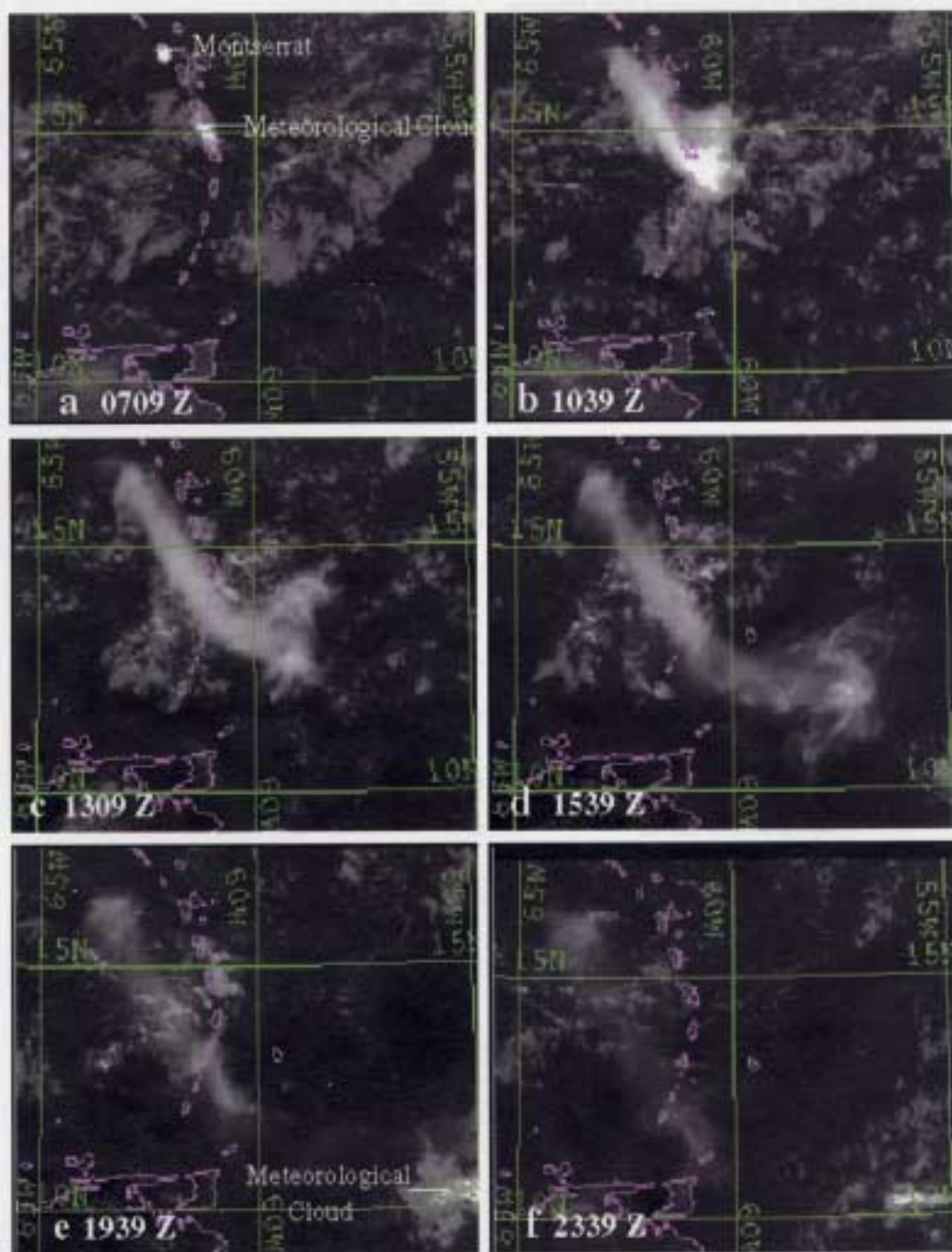


Fig. 3. Selected GOES hand 4 volcanic cloud images, 26 December 1997. The volcanic cloud starts out as a bright spot, reflecting a very low brightness temperature and high opacity; with time the cloud grows in size but dims in contrast as it becomes more transparent.

this was corrected using wavelength-dependent data collected by Pollack *et al.* (1973). We retrieved volcanic cloud information in two parts, to allow for differing cloud heights. Cloud heights were constrained by wind trajectory data. The area of the volcanic cloud in band 4 images was measured to compare them with areas of the ash in the volcanic cloud shown in the BTM images (Fig. 2). This procedure is subjective and was done to estimate any underestimation of ash mass in the volcanic cloud due to the tropospheric moisture.

GOES and AVHRR results

Band 4 brightness temperatures. GOES 8 collected 33 images of the volcanic cloud on 26 December 1997, approximately every 30 minutes from 07:09 universal time (UT; 03:09 local time) (*c.* 8 minutes after the eruption began), until 23:39 UT. The pattern of movement of the volcanic cloud is shown by six selected band 4 images in Figure 3. The volcanic cloud cannot be distinguished from meteorological clouds in band 4, but this type of representation does show the overall pattern of dispersal well, and it displays the full size of the cloud, even after the infrared ash signal is too weak to be detected. Throughout the *c.* 17 hours shown in Figure 3, the volcanic cloud was elongated hundreds of kilometres to the SE, while simultaneously migrating 120 km to the SW (from the volcano to the cloud centroid). The first image (Fig. 3a) shows a sharply defined volcanic cloud, with a high optical depth reflected in the cold temperature, located near the volcano with an area of 770 km², and elongated 40 km to the SE. The cloud ultimately rose to *c.* 15 km, based on comparing radiosonde data from the Guadeloupe weather station (Fig. 4) and the cloud brightness temperatures (200 K) derived from band 4 data of high-optical-depth pixels of the cloud in the two earliest images (07:09 UT and 07:39 UT; the latter is not shown in Fig. 3). The radiosonde data (Fig. 4) show that the temperature was 200 K at two altitudes: in the troposphere at *c.* 15 km, and in

the stratosphere at *c.* 20 km. Wind-trajectory analyses show that the volcanic cloud did not rise to 20 km, therefore *c.* 15 km was the maximum altitude that the volcanic cloud reached.

BTM retrieval results. Figure 5 shows the volcanic cloud as discriminated by BTM. Figures 2 and 3 show how the area of the volcanic cloud changed with time during 26 December. It increased in size rapidly at first, slowing and reaching a maximum at about 16:00 UT and then slowly decreased in size. The band 4 areas of the cloud were larger by about an order of magnitude during much of the day. The difference in areas occurred in part because the 26 December 1997 dome collapse was smaller than other eruptions shown in Figure 1, so the concentration of fine ash in much of the volcanic cloud was not high enough for the sensor to detect. The volcanic ash signal for each pixel must be strong enough to override the effects of any hydrometeors in the volcanic cloud, or the effects of high humidity depressing infrared radiation transmission in the tropical lower troposphere (Coll & Caselles 1997).

Figure 6 summarizes the time trends of the 26 December 1997 volcanic cloud, including mass, area and mean optical depth. This represents the BTM-determined ash-rich core of a larger cloud. The two-dimensional shapes of these cloud cores are shown in Figure 5. Retrieval results from GOES 8 are given in Table 2. Between 07:39 and 09:39 UT the volcanic cloud area decreased by 40%, and total ash mass of the volcanic cloud decreased by 75% (Fig. 6). These decreases were probably caused by interference of the transmission of the ash signal to the sensor by a VM cloud. The times when the volcanic cloud ash signal was masked by the VM cloud is shown in Figure 6. After 09:39 UT the total area and silicate mass increased until 16:39 UT and 13:09 UT, respectively, with a general decrease thereafter. The optical depth decreased rapidly after 09:39 UT until 13:39 UT, when it began to decrease at a slower rate. The maximum mass of fine ash (45×10^3 kg) was detected at 07:39 UT, *c.* 38 minutes after the explosive activity began. The volcanic cloud core

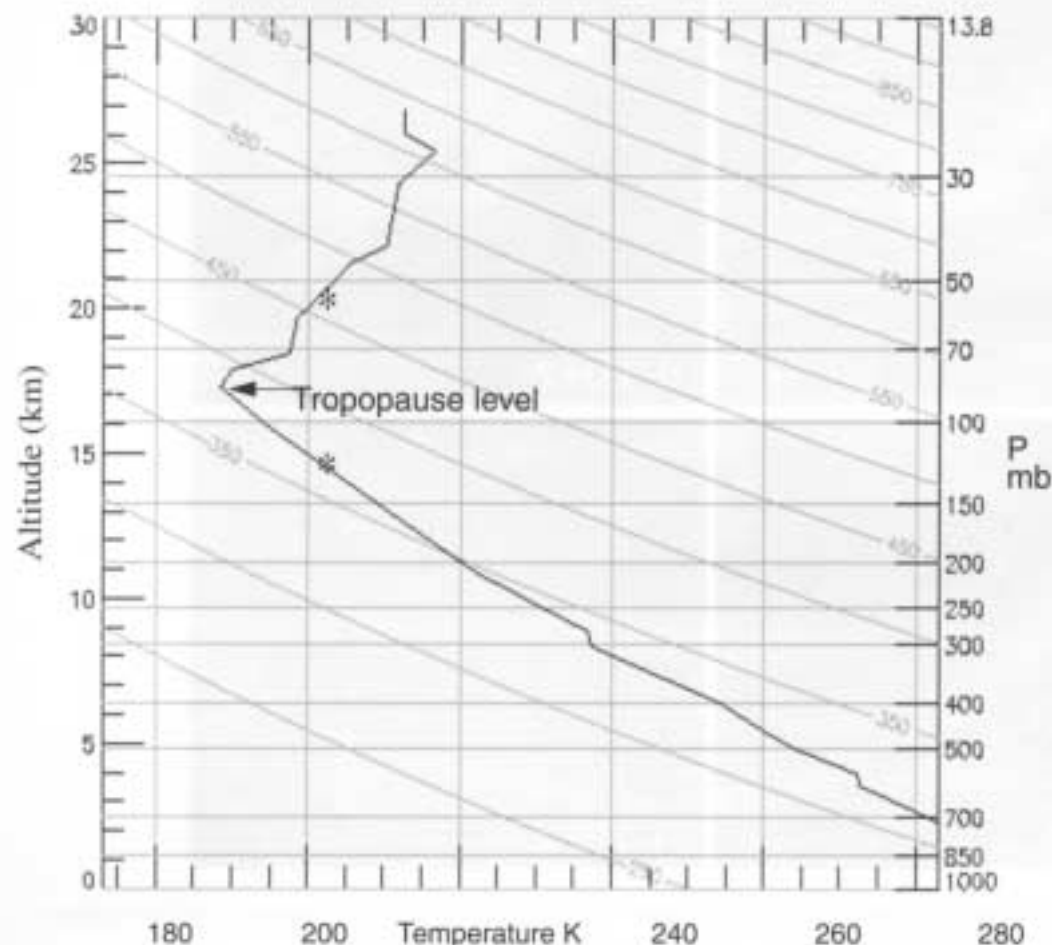


Fig. 4. Upper atmosphere temperature profile at 11:00 UT at Guadeloupe. Asterisks indicate the two altitudes where the temperature was 200 K. Pressure (*P*) in millibars.

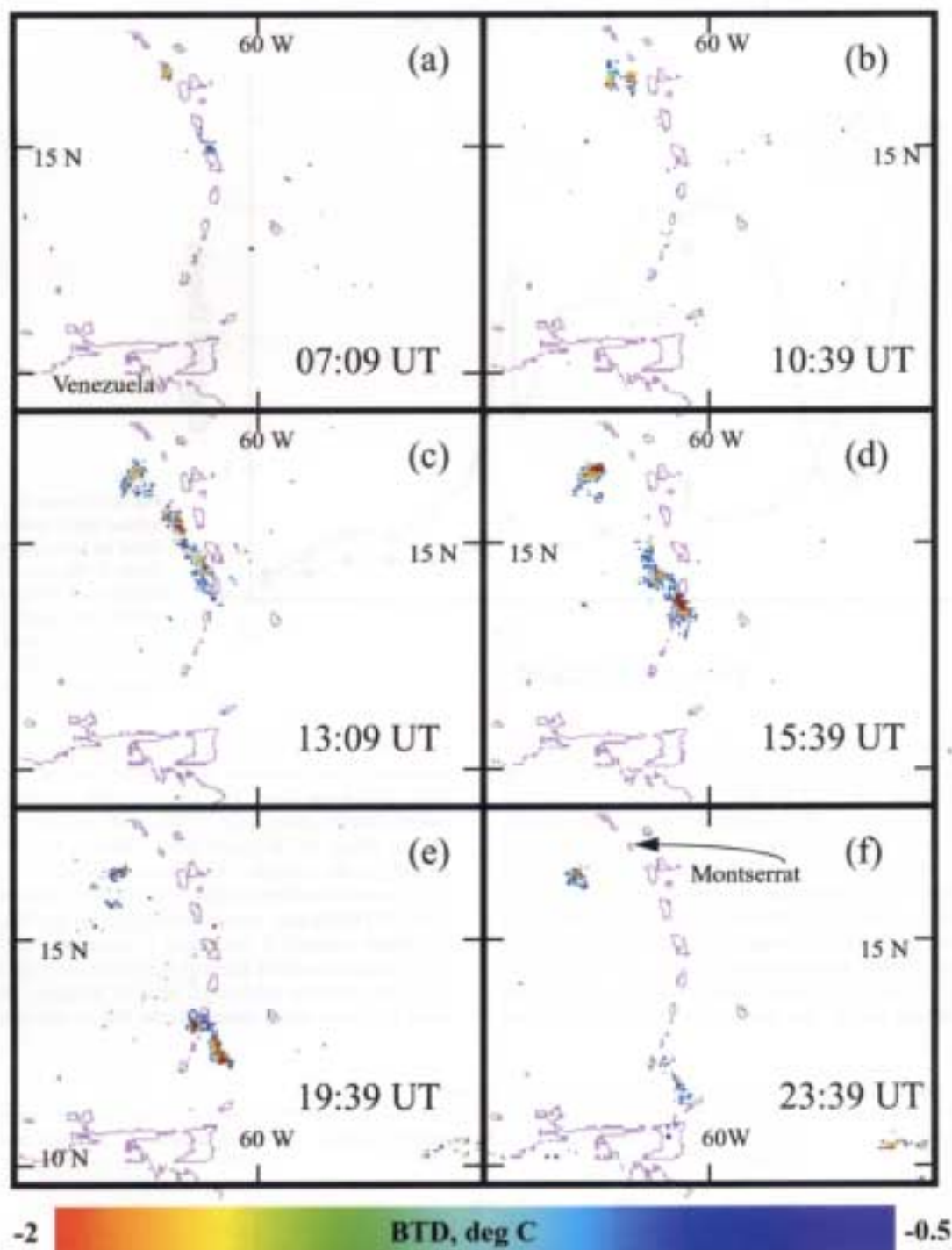


Fig. 5. Selected GOES brightness temperature difference (BTD) images, 26 December 1997. The size of the volcanic cloud as outlined by BTD is much smaller than that outlined by band 4 (Fig. 3), as only the dense cores of the cloud, richer in volcanic ash, are detected by cutoff values less than -0.5 K for BTD.

as seen with BTD data expanded to 16 times its size in the first image (Fig. 5a) over 11.6 hours to a maximum area of 8000 km^2 (Fig. 5d).

Figures 7 and 8 show the spatial distribution of the cloud optical depth, fine ash mass and mean effective radius (Table 2). The algorithm used in the retrieval model produces masses derived from the optical depth; therefore they are directly related (Fig. 7). The cloud's overall highest ash mass and optical depth occurred in the first hour after the onset of the explosive activity (07:39 UT), when the cloud had an average optical depth of 2.6 and was partially opaque (optical depth >4). The mass and optical depth generally decreased until 15:39 UT although they increased slightly in the northern section of the volcanic cloud beginning at 13:09 UT.

AVHRR results. A single NOAA 14 AVHRR image from 17:47 UT on 26 December 1997 was also analysed (Fig. 6) by the same algorithm and tabulated with the GOES data in Table 2.

Total Ozone Mapping Spectrometer (TOMS)

TOMS is an ultraviolet spectrophotometer that operates in a polar sun-synchronous orbit on board NASA's Earth Probe (EP) satellite. TOMS compares spectral radiance of the sunlit atmosphere with radiance of a sunlit calibrated diffuser plate from a satellite platform (Krueger *et al.* 1995). EP/TOMS has a 2100 km swath

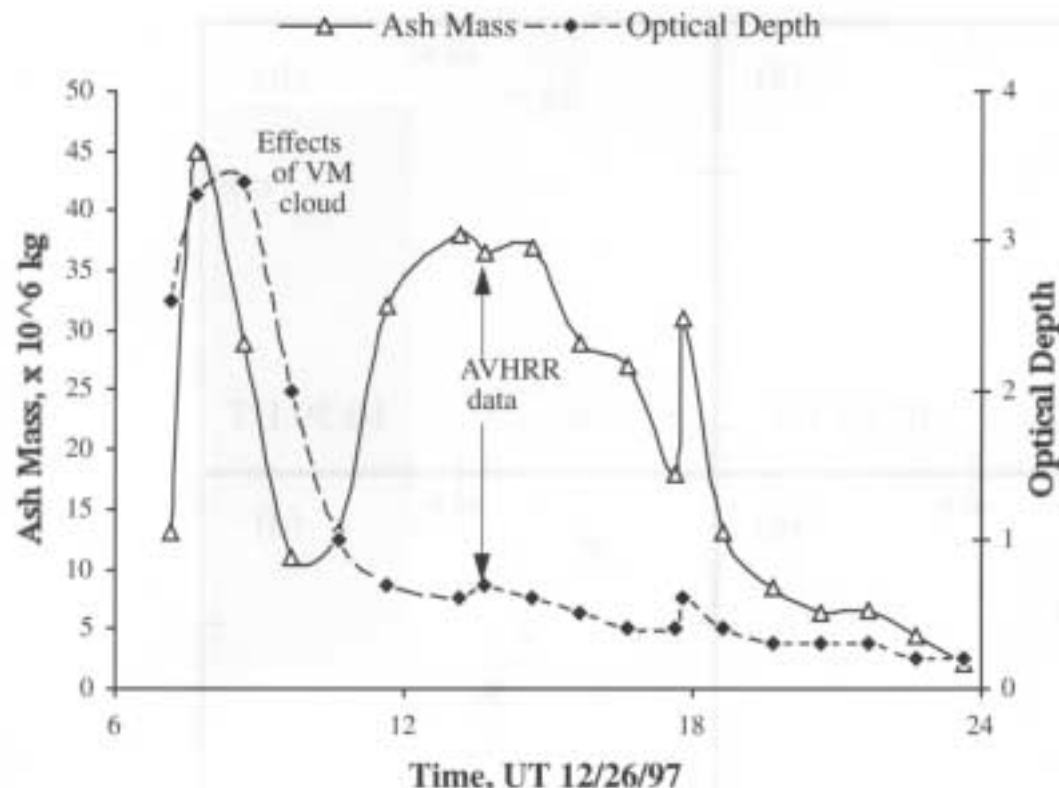


Fig. 6. Changes in fine ash mass, and optical depth (unitless) of the volcanic cloud on 26 December 1997. Data from Table 2. The two AVHRR points are labelled; all of the others are from GOES. The points between about 8 and 12 UT (shaded area) are during the period of masking effects of the volcanogenic meteorological cloud.

and 90% Earth coverage; it images the same area once daily, with 39 km pixel size at nadir (McPeters *et al.* 1998). Four bands within the 312–380 nm region are used to determine total-column SO_2 loadings (Krueger *et al.* 1995). SO_2 concentrations are measured in Dobson units (DU), which represent the thickness of gas at standard temperature and pressure that affects the reflection of ultraviolet radiation in a column that extends from the satellite to the reflective surface. A data visualization software package (IDL) program developed by NASA (Krueger *et al.* 1995) calculates the total concentration of SO_2 by multiplying the DU of SO_2 in each pixel collected by TOMS by the area of the pixel and a conversion factor, then summing all of the pixels in the area of interest

(Krueger *et al.* 1995). The algorithm used in the program compares radiance values collected by TOMS with pre-computed radiances from a look-up table. The look-up table includes the 26 standard ozone profiles and a layer of SO_2 with amounts from 1 DU to 600 DU at 20 km (N. Krotkov, pers. comm.). The total concentration of SO_2 in the volcanic cloud was corrected for background levels (i.e. sensor-dependent levels) of SO_2 (after Constantine *et al.* 2000). The EP/TOMS data are not rectilinear, so the SO_2 located between the pixels scanned is calculated by assuming that the area of SO_2 in the cloud missed by the scan is a function of the ratio between the scan area and the total cloud area (S. Schaefer, pers. comm.). The final SO_2 mass value represents the SO_2 in the cloud, including SO_2

Table 2. GOES and AVHRR infrared volcanic ash retrieval results

Time (UT)	No. of ash pixels	Cloud area (km^2)	Mean effective radius (μm)	Mean optical depth	Fine ash mass ($\times 10^6$ kg)
07:09	35	560	7.0	2.6	13
07:39	79	1300	8.3	3.3	45
08:39	48	770	8.6	3.4	29
09:39	48	770	5.6	2.0	11
10:39	113	1800	5.7	1.0	13
11:39	291	4700	7.7	0.7	32
13:09	403	6500	7.6	0.6	38
13:39	354	5700	6.7	0.7	36.5
14:39	460	7400	6.7	0.6	37
15:39	451	7200	6.2	0.5	29
16:39	503	8000	6.0	0.4	27
17:39	372	5900	5.2	0.4	18
17:47*	451	8700	5.0	0.6	31
	(7217)*				
18:39	222	3600	4.8	0.4	13
19:39	318	5100	5.0	0.3	8.5
20:39	284	4500	4.3	0.3	6.4
21:39	257	4100	4.7	0.3	6.5
22:39	243	3900	4.2	0.2	4.4
23:39	126	2000	4.0	0.2	2.2

* AVHRR data have smaller pixels (higher spatial resolution) so an equivalent number is calculated to compare. Data from Wen & Rose (1994). Mean optical depth is unitless. Local time = universal time (UT) minus 4 hours.

between the scanned pixels but excluding background values, with an approximate error of $\pm 30\%$ (Krueger *et al.* 1995).

In addition, the aerosol index (AI) is mapped from TOMS data. AI is a unitless, relative scale that identifies relative amounts of aerosols and ash in volcanic clouds (Seftor *et al.* 1998). AI is the difference in the logarithms of backscattered radiance at two near-

ultraviolet wavelengths compared with what would be expected for a pure Rayleigh atmosphere over a Lambertian surface (Krotkov *et al.* 1999). Meteorological clouds have AI values of approximately 0 while absorbing media (ash clouds, smoke and dust) have positive values that increase with higher optical depth (a maximum value of 6 was used in this study). The practical application of the AI

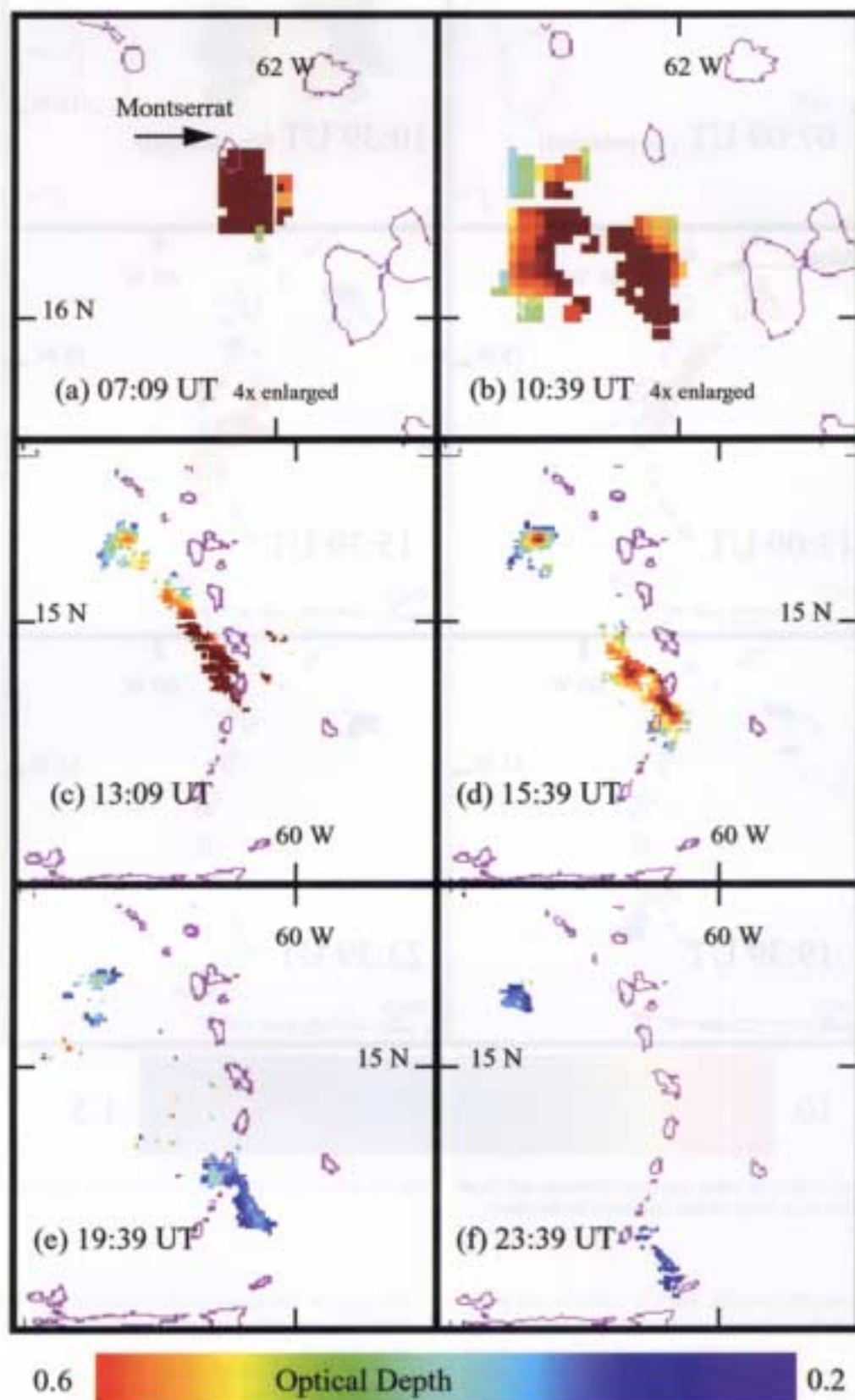


Fig. 7. Spatial distribution of optical depth values (unitless) within the volcanic cloud cores for selected data, 26 December 1997. The first two images are enlarged in scale by a factor of four compared to the others.

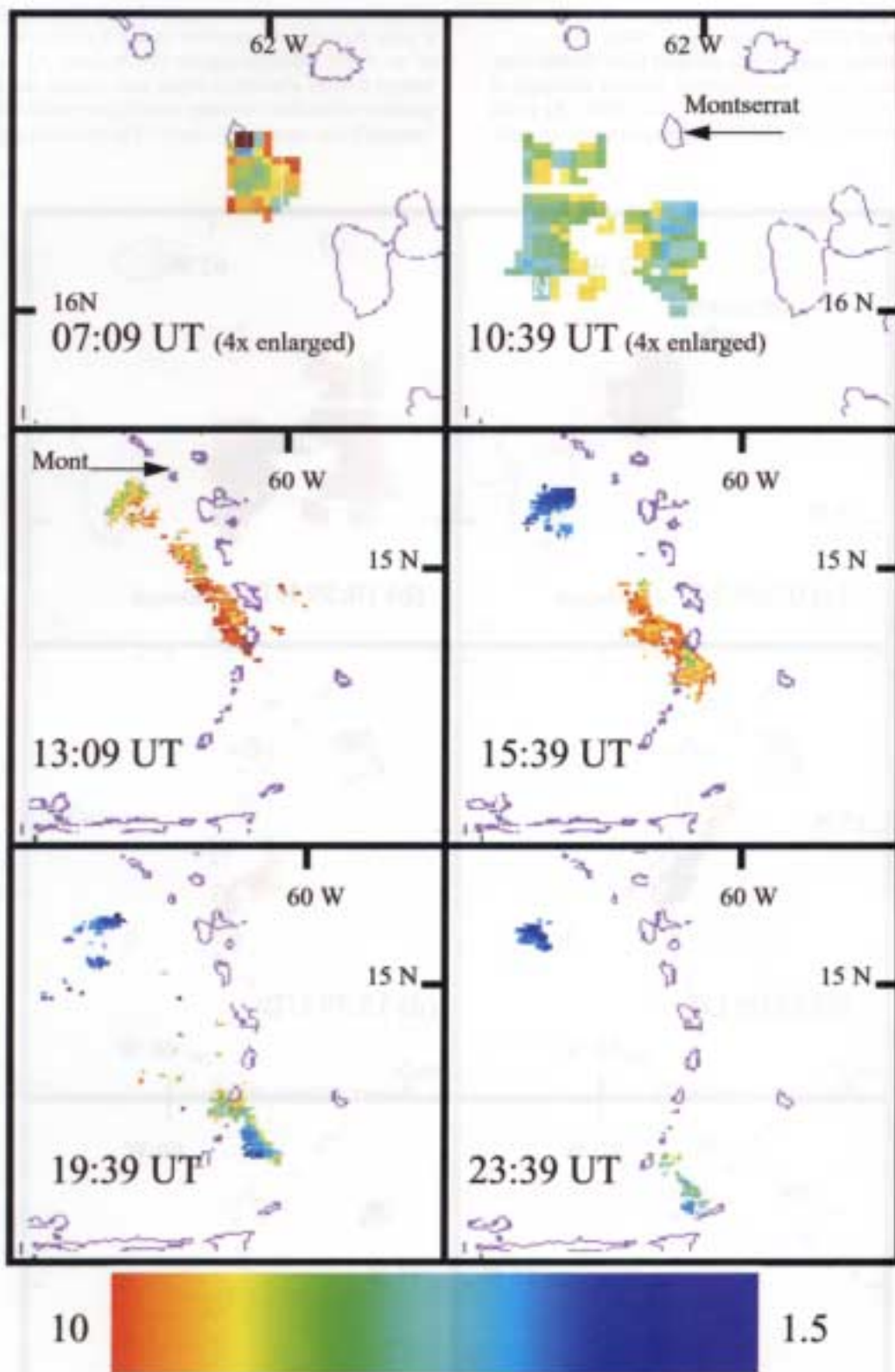


Fig. 8. Spatial distribution of effective radius retrievals of volcanic ash (in μm) within the volcanic cloud cores for selected data 26 December 1997. The first two images are enlarged in scale by a factor of four compared to the others.

scale to cloud analysis can be complex, but it is similar to the infrared retrievals of Wen & Rose (1994). As shown by Krotkov *et al.* (1999, fig. 2), an AI value for a given particle size distribution can be considered linearly related to ash optical depth (hence mass) under typical cloud conditions. Thus, for a mean effective radius of $1 \mu\text{m}$, an AI value of 10 would represent approximately twice the mass of an AI value of 5. For other mean effective radii, the relationship is still roughly linear, but not necessarily one-to-one. However, if

the particle size distribution is multimodal, the AI/mass relationship also becomes a function of multiple curves (one for each size distribution).

One TOMS observation of the volcanic cloud is available at 15:43 UT (Figs 9 and 10), nearly coincident with the areal maxima for the volcanic cloud and with one of the GOES data sets. The swath that captured the volcanic cloud terminated at the SE edge of the cloud (Fig. 9), so the SO_2 mass of $340 \times 10^6 \text{ kg}$ is a

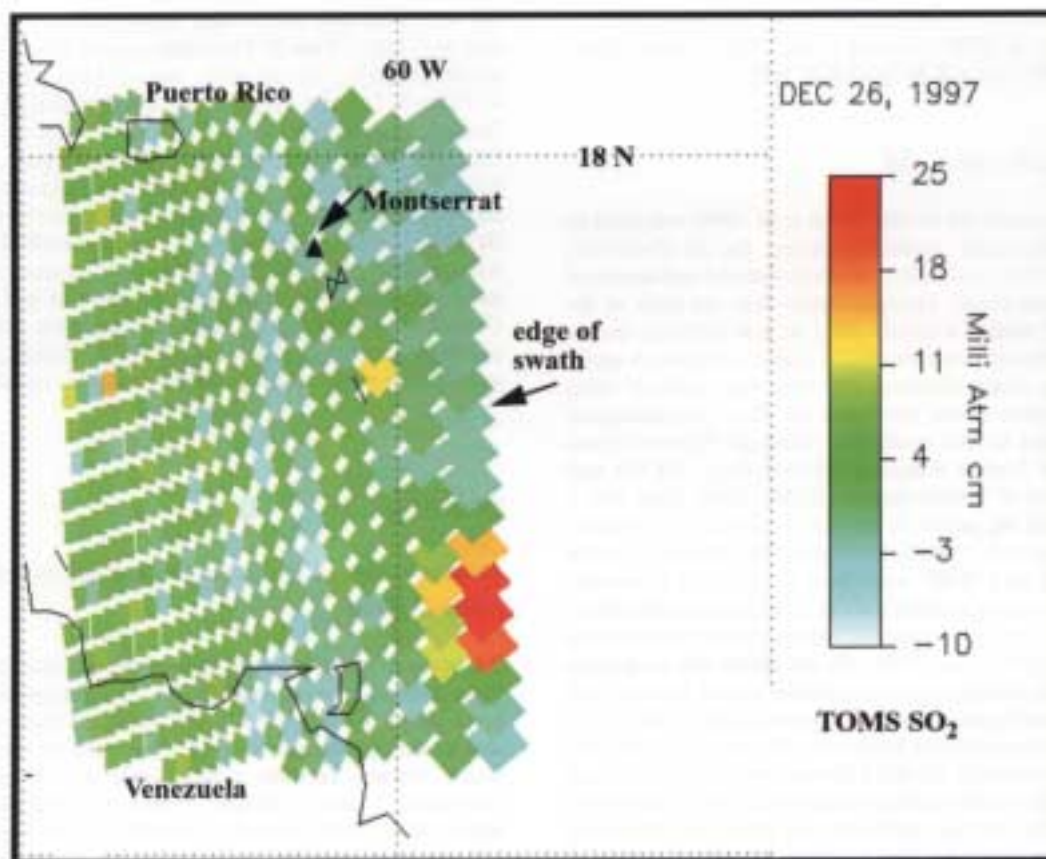


Fig. 9. TOMS SO_2 cloud at 15:43 UT, 26 December 1997. In this plot the footprints of individual pixels are plotted with their SO_2 burden in Dobson units (equivalent to milli-atm cm and shown by colour scale). Note that the east edge of the SO_2 cloud is undefined because of the edge of the orbital swath.

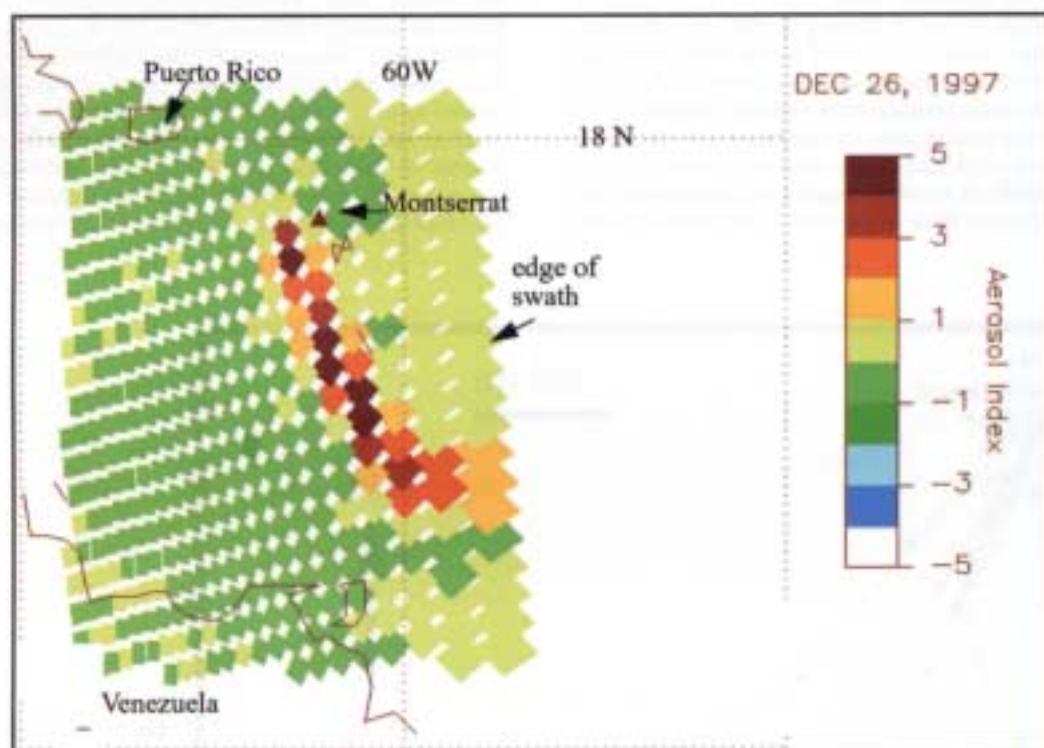


Fig. 10. TOMS aerosol index (AI; unitless) map at 15:43 UT, 26 December 1997. Note that the AI image shows an elongate volcanic cloud, with a very different shape from the SO_2 (Fig. 9).

minimum value. The TOMS AI map (Fig. 10) located ash south of Montserrat with an area of $c. 150\,000\text{ km}^2$ (about 30% larger than the band 4 area in Fig. 3) and elongated towards the SSE. The ash extended from west of Montserrat to the SSE until $c. 60^\circ$ west and then continued east creating a hook shape that is also con-

spicuous in the 10:39 UT and 13:09 UT GOES 8 band 4 images (Fig. 3b and c). This comparison shows clearly that the ideal TOMS AI data, collected at solar noon, can outline the volcanic ash much more fully than GOES or AVHRR data. Note that the SO_2 was located in the easternmost portion of the volcanic cloud. Separation

of SO₂ and ash in volcanic clouds has been observed in a number of other cases (Rose *et al.* 1995; Holasek *et al.* 1996; Shocker 1996; Schneider *et al.* 1999) and will be discussed below.

Isentropic wind trajectory model

An isentropic wind trajectory model (Allen *et al.* 1999) was used to recreate the meteorological conditions during the 26 December, 1997 collapse in an effort to simulate the three-dimensional dispersal of ash in the volcanic cloud. Meteorological data are poor in the tropics because the weaker Coriolis effect at low latitudes causes wind dynamics to be more complex than at higher latitudes. A qualitative reconstruction of ash dispersal over time was produced using wind data. Five models of the wind data by three meteorological centres were analysed in this study: the National Meteorological Center (NMC), the United Kingdom Meteorology (UKM) and the American Society of Meteorologists (ASM). NMC data with a 1° × 1° grid produced the model of the volcanic cloud that visually correlated most accurately with the position of the volcanic cloud in GOES 8 imagery. Using NMC wind field data for 26 December 1997, the model was run by starting a set of 72 air parcels distributed in a 25 km diameter ring centred on the volcano when the explosive activity began (Schoeberl *et al.* 1992). In the model the air parcels are advected by wind, temperature and pressure values derived from NMC's balanced wind equations and then interpolated to isentropic (constant potential temperature) levels over the length of time the volcanic cloud was visible by GOES 8 (Schneider *et al.* 1999). Data are available every six hours starting at 06:00 UT on 26 December 1997 (*c.* 1 hour prior to the collapse) and they were averaged between the six-hour intervals. The positions of the air parcels at various heights were compared to the position of the volcanic cloud in band 4 and BTD GOES 8 images to determine the vertical extent of the volcanic cloud.

The isentropic wind trajectory model was run for a range of altitudes starting at 07:00 UT on 26 December 1997 with all points initially located at the volcano. Trajectory points were computed for air parcels at different altitudes at four-hour intervals (Fig. 11). The trajectory points were compared to satellite images of the volcanic and VM clouds to determine the matching altitude. From comparing positions of the parcels in the trajectory results and the orientation of the clouds in satellite imagery, we discovered that the volcanic cloud extended from about 2 to 15 km altitude, while

the VM cloud rose to *c.* 17 km. Wind trajectory data (Fig. 11) show that by 12:00 UT on 26 December ash at 2 km altitude had travelled at 24 km h⁻¹ to the west, ash at 4 km altitude had travelled at 15 km h⁻¹ to the SW, and ash at 6 km altitude had travelled at 26 km h⁻¹ southward. At altitude of 8 km and above the ash moved SE; the wind speed was 41 km h⁻¹ at 8 km and increased to 72 km h⁻¹, 104 km h⁻¹ and 109 km h⁻¹, respectively at 10 km, 12 km and 14 km altitudes. At 16 km the wind speed slowed to 70 km h⁻¹. By 00:00 UT on 27 December 1997 wind speeds at 12 km and 14 km were similar (98 km h⁻¹ and 85 km h⁻¹, respectively) and in the same direction (SE), causing co-location of ash at these heights. Overall wind speeds increased from 2 to 14 km altitude at 12:00 UT and from 2 to 12 km altitude at 24:00 UT. Thus in general the higher parts of the cloud travelled farther from the volcano.

Discussion

Determination of the three-dimensional morphology of the volcanic cloud

Three-dimensional visualization of the volcanic cloud was derived from combining our observations. The conspicuous SSE-pointing hook shape in the 10:39 UT and 13:09 UT band 4 images (Fig. 3b and c) can be explained by the trajectory of the wind. The hook shape formed because wind speeds at an altitude of 14 km (109 km h⁻¹), and at 16 km (70 km h⁻¹), were slower than speeds below them (13 km altitude, 119 km h⁻¹), and because before 13:09 UT winds at altitudes above 14 km blew in a slightly (15°) more easterly direction. A cross-sectional view of the volcanic cloud trajectory showing the latitude of ash at various heights was created from wind trajectory data (Fig. 12). The plot shows the position of the volcanic cloud 24 hours after the eruption began, with the wind field data averaged between 00:00 UT on 26 December 1997 and 00:00 UT on 27 December 1997. By *c.* 07:00 UT on 26 December the wind speed gradually increased up to *c.* 9 km altitude, then decreased up to *c.* 12 km, and then increased again causing the volcanic cloud to have an S-shaped front. This is significant because, in the absence of wind shear, the satellite would see overlapping layers of fine ash at the same latitude. The wind direction on 26 December 1997 was constantly to the SE (with azimuth varying <15°) between

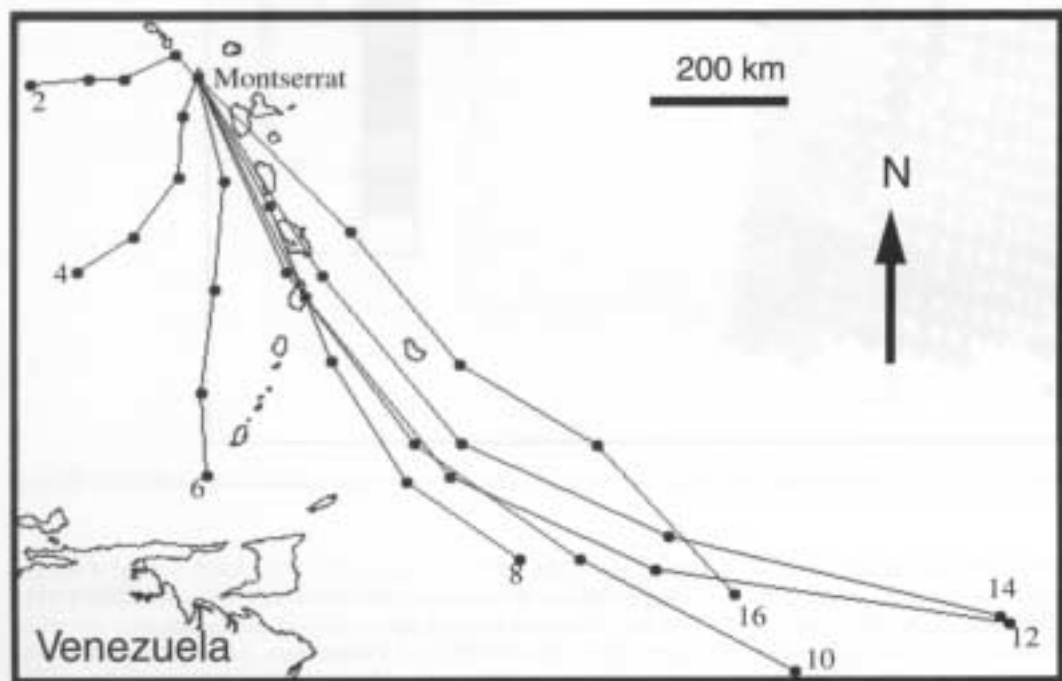


Fig. 11. Isentropic trajectory model results for 26 December 1997. Each line connects points of parcels moving at equal altitudes of 2, 4, 6, 8, 10, 12, and 14 km. Points represent 4 hours of movement. All sets begin at the volcano at 06:39 UT and include 10:39, 14:39, 18:39 and 22:39 UT, with each point being farther from the volcano's position reflecting continued movement by winds.

c. 8 km and 16 km altitude, with little wind shear, thus overlapping layers were seen by the satellite sensors. This three-dimensional visualization of the cloud helps us evaluate whether the assumption of cloud shape parallel to the Earth's surface is violated seriously.

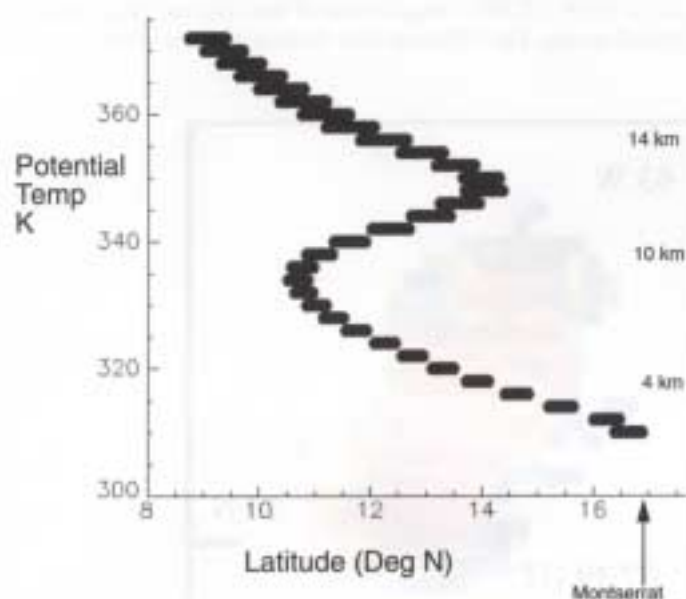


Fig. 12. A cross-sectional north-south view of dispersed volcanic cloud parcels at 07:00 UT on 27 December 1997, 24 hours after the start of the eruption. The plot is meant to show how the cloud's trajectory at different altitudes led to an overlapping relationship. The vertical axis is plotted in a meteorological format, with potential temperature (left) and actual height (right).

Because the cloud's slope towards the upwind direction is slight (rise of c. 10 km in a run of c. 800 km), it is very nearly parallel.

Comparison of satellite retrieval data

We compared similar volcanic cloud data from two satellites. Figure 13 shows the correlation of the AVHRR and GOES 8 images. The GOES 8 image was collected about 8 minutes before the AVHRR image and as a result the contours showing the ash position determined from GOES 8 data are shifted about 7 km NE of the position of the AVHRR ash cloud. Wind speeds reached a maximum of 119 km h^{-1} at 13 km altitude and the average speed between 2 and 15 km was 51 km h^{-1} , so the ash in the AVHRR image had been moved by wind during the time between data collections (7 km, 8 minutes, c. 52 km h^{-1}). Retrievals for both data sets are compared in Table 2. Correcting for differing pixel resolutions, the area of volcanic cloud detected by AVHRR is 47% higher than GOES. The mean optical depth retrieved by the AVHRR is also higher by 47%, and these differences result in the ash mass being 81% higher. These differences are most likely caused by the higher spatial resolution of the LAC AVHRR data, which results in a larger footprint of ash cloud, resulting from the addition of pixels at the optically thin fringes (i.e. BTD close to -0.5°C).

The volcanogenic meteorological cloud associated with the 26 December event

The pattern of movement of the VM cloud, which we believe formed from the evaporation of seawater by the pyroclastic density current with seawater (see discussion below), was revealed by the

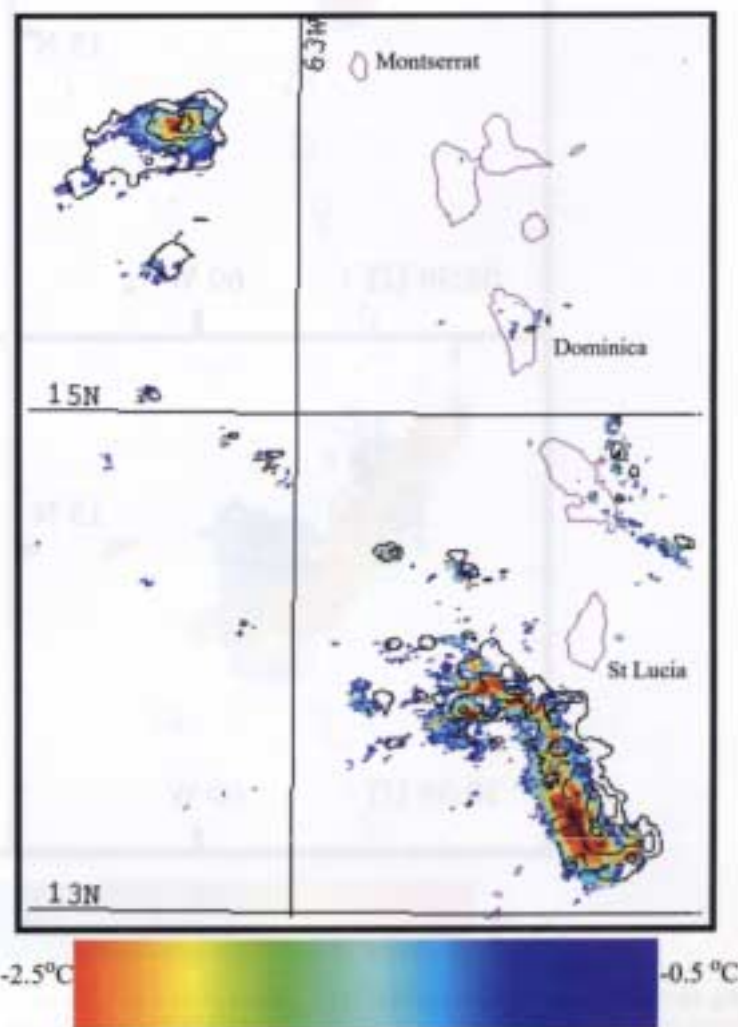


Fig. 13. Comparison of the position of brightness temperature difference (BTD) volcanic cloud anomalies from GOES 8 (17:39 UT) and AVHRR (17:47 UT). The GOES data are contoured with black lines at $\text{BTD} = -0.5, -1.5, -2.5 \text{ K}$. The slight positional offset of the cloud position is explained by the time differences and the prevailing winds.

GOES 8 data. Part of the 26 December volcanic cloud had high ($>5^{\circ}\text{C}$) positive BTD values, unlike most other studied volcanic clouds (Shannon 1996; Constantine *et al.* 2000; Schneider *et al.* 1999). The positive BTD values were observed from 07:09 UT to 11:39 UT (Fig. 14). While volcanic clouds typically have negative BTD values (red and orange in Fig. 14), and the lowest meteorological clouds have positive BTD values between $c. 0$ to 5°C (green and

yellow), in this case a portion of the volcanic cloud had BTD values $>5^{\circ}\text{C}$ (blue). These blue regions show the signal of the VM cloud dominates. The high BTD values reflect the presence of ice and liquid water, rather than ash. As Figure 14 illustrates, at 07:09 UT pixels $>5^{\circ}\text{C}$ were concentrated west of the volcanic cloud, and at 07:39 UT they fringed most of the volcanic cloud and increased in area. The VM cloud then masked portions of the volcanic

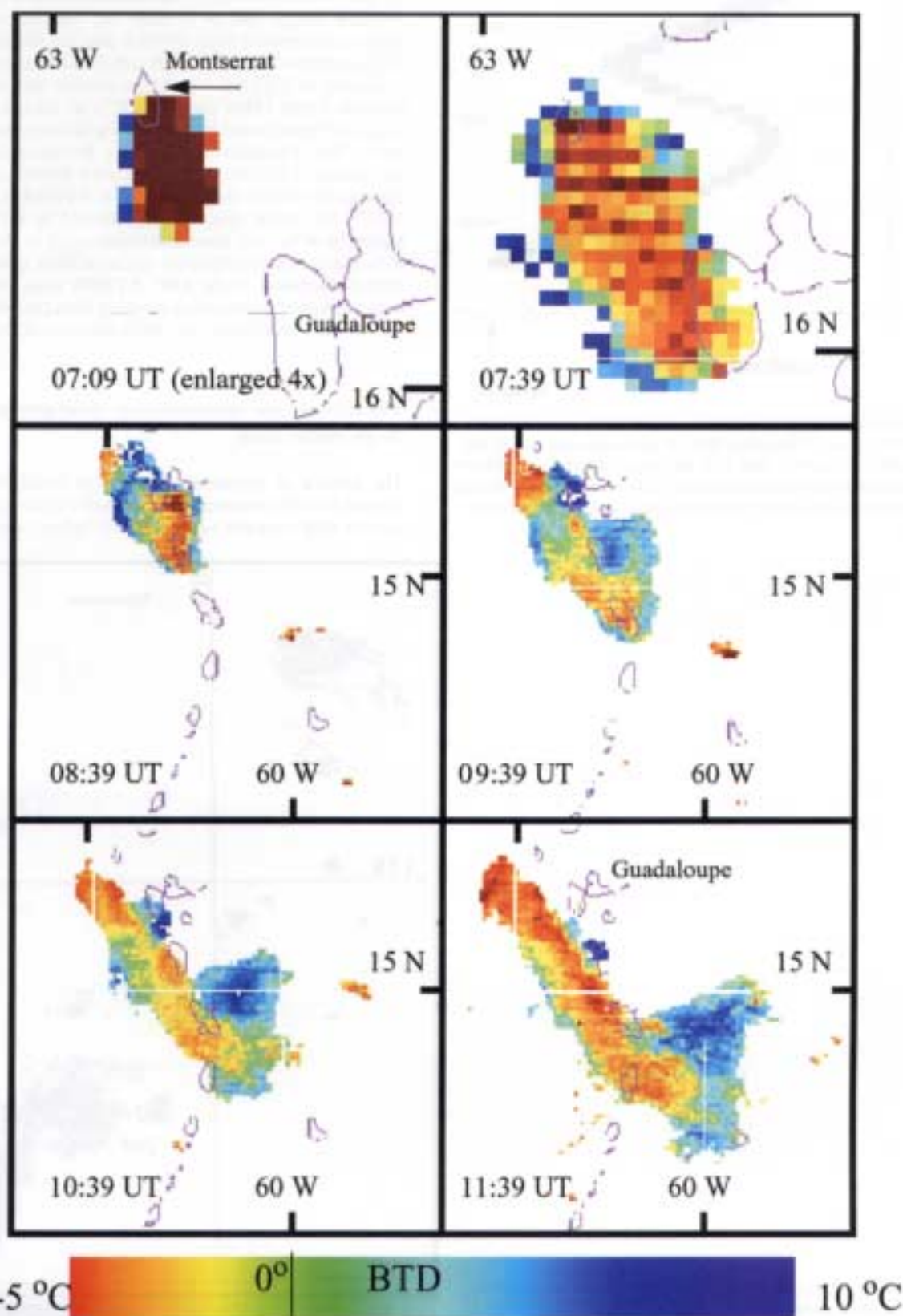


Fig. 14. Selected GOES images, highlighting the position of the volcanic cloud and the volcanogenic meteorological (VM) cloud, 26 December 1997. Red and brown pixels depict the volcanic cloud ($\text{BTD} < -0.5$) while blue pixels depict the VM cloud ($\text{BTD} > 0$).

cloud until 11:39 UT. The VM cloud is generally located along the northern fringe of the volcanic cloud near the leading edge (Fig. 14).

Modelling of the microphysics in volcanic clouds shows that ice is the dominant phase at $c. 6$ km in altitude where temperatures are generally less than -40°C (Herzog *et al.* 1998). Thus the VM cloud was most likely composed primarily of water below 6 km and ice above 6 km. The volcanic cloud from the eruption of Rabaul in 1994 was shown to have abundant ice (Rose *et al.* 1995) and this was derived from seawater entering the vent rather than external seawater/density current interactions. The ice in the Rabaul cloud produced highly positive BTD values in AVHRR images, which masked the characteristic spectral signature of the ash in a similar manner.

The VM cloud masks the characteristic spectral signature of ash in the volcanic cloud by dampening the negative BTD value of the ash pixels with the highly positive BTD meteorological cloud pixels. The satellite detects upwelling thermal radiation that is scattered and absorbed by clouds, and in this case detects effects of both hydrometeors (snow, hail, graupel and raindrops) and volcanic ash. One assumption of the Wen & Rose (1994) retrieval method – that the atmosphere above and below the volcanic cloud is clear – is violated in this case. The masking effect of the VM cloud is evident on plots of the volcanic cloud's physical characteristics (Fig. 6). The masking effect was most prominent between 07:39 UT, when the meteorological cloud rose high enough to disturb the characteristic spectral signature of the ash, and 13:09 UT, when it began to dissipate.

Although the 26 December 1997 collapse was not directly observed, the idea that the VM cloud resulted from interaction between the pyroclastic density current and seawater is supported by observations and photographs of smaller Soufrière Hills volcanic events, particularly the 12 May 1996 dome collapse. The pyroclastic flow on 12 May 1996 involved $0.4 \times 10^6 \text{ m}^3$ of dome material that descended Tar River valley (Cole *et al.* 2002). It travelled to the sea where the upper surge component detached and travelled 200 m across the sea surface, while the dense basal avalanche entered the

sea (Cole *et al.* 2002). The flow front velocity increased from $8\text{--}15 \text{ m s}^{-1}$ to a maximum of 25 m s^{-1} . Lofting ash plumes were seen above the distal end of the flow and boiling water near the pyroclastic fan produced dense steam that rose several hundred metres (Cole *et al.* 2002).

Information about the hydrometeors in the VM cloud was retrieved from the 09:39 UT GOES 8 image (when the VM cloud had its highest optical depth) using the model of Wen & Rose (1994) and following the same methodology as Rose *et al.* (1995) used in the analysis of the ice in the Rabaul volcanic cloud. The VM cloud was $10\,000 \text{ km}^2$ and the mean effective radius of its ice was $24 \mu\text{m}$. The total mass of ice in the VM cloud was thus estimated from the remote sensing data at $1.5 \times 10^9 \text{ kg}$, which is $c. 3.5$ times the mass of the silicate ash in the volcanic cloud ($4.5 \times 10^7 \text{ kg}$).

Without other data the imagery cannot resolve whether the VM cloud underlies, overlaps or overlies the volcanic cloud. The VM cloud had its largest area at 10:39 UT ($12\,000 \text{ km}^2$) and, based on wind trajectory data, one part of the VM cloud was higher than the volcanic cloud, at a height of 16 km or more (Fig. 15). The range of trajectory-based heights for the VM cloud go from about 4 to perhaps 17 km. At 10:39 UT there appears to have been a slower-moving, lower (4–8 km altitude) part of the VM cloud south of Guadeloupe and west of Dominica, and a higher (8–17 km altitude) part located to the east of Martinique and St Lucia. By 11:39 UT the northern section of the VM cloud dissipated and the southern portion increased in area towards the east. After 11:39 UT the remaining portion of the VM cloud continued to dissipate until it was below satellite detection limits by 13:39 UT, while the volcanic cloud remained detectable. The evolution of the VM cloud is shown schematically in Figure 16.

Dissipation of the VM cloud coincided with local noon (16:00 UT) on Montserrat, so its disappearance may be associated with increasing solar radiation of a surrounding undersaturated atmosphere. Also, as Rose *et al.* (1995) proposed for Rabaul, the presence of ice in the volcanic cloud may have reduced the residence time of

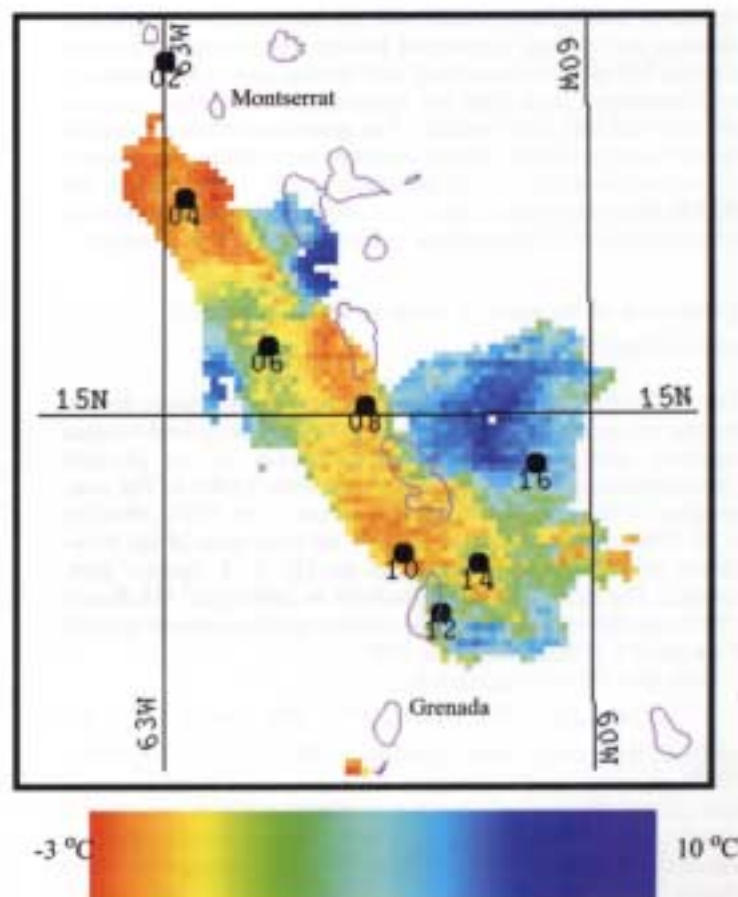


Fig 15. Trajectory data (from Fig. 11) at 10:39 UT (black dots with numbers represent altitude in km) superimposed over the 10:39 UT brightness temperature difference map from Fig. 13.

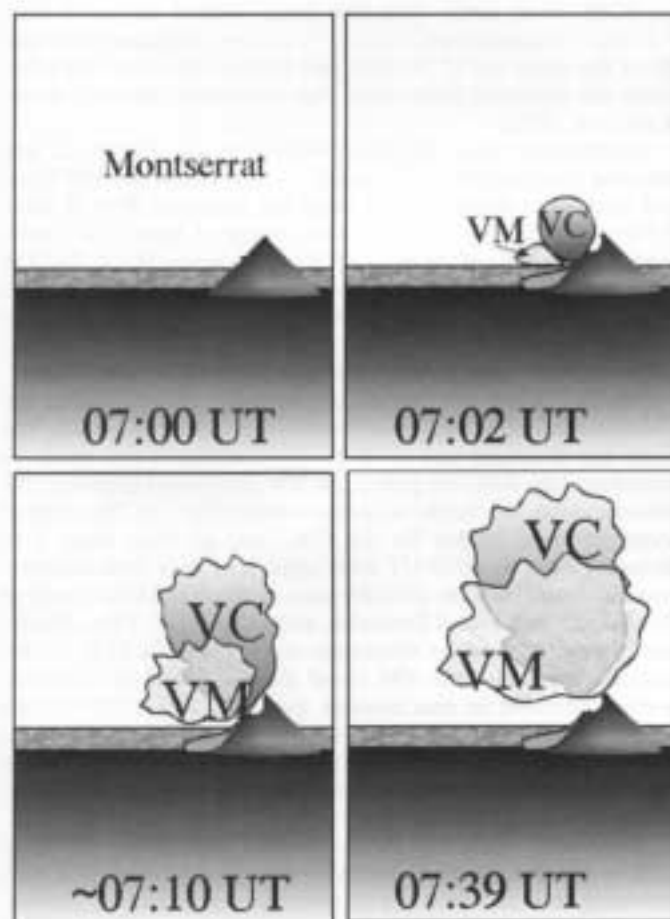


Fig. 16. Schematic cross-sectional diagram of the clouds of 26 December 1997, as seen looking north at various stages in the first hour beginning at 07:00 UT (VC, volcanic cloud; VM, volcanogenic meteorological cloud).

the ash by coating the particles with ice, increasing their mass and diameter and causing accelerated fallout. The accretionary lapilli deposits SW of the volcano may have formed due to hydrometeor/ash interactions soon after the eruption, but before the volcanic cloud drifted SSE of the volcano. The generation of meteorological clouds from pyroclastic density currents that reach the sea is likely to have occurred often in the geological record, for example in the 1883 Krakatoa eruption (Carey *et al.* 1996), and could represent an important means of atmospheric perturbation by large eruptions.

Estimation of the mass of water in the volcanogenic meteorological cloud

The maximum mass of water evaporated by the pyroclastic density current upon entering the sea can be estimated using heat-balance equations and constrained using information on the physical characteristics of the VM cloud retrieved from GOES 8. The temperature of the andesitic magma is known to be 850°C (Barclay *et al.* 1998), and an estimated 85% of the total mass of the pyroclastic density current reached the sea (R. S. J. Sparks, pers. comm.). The density of dense andesite is 2600 kg/m³ (McBirney 1993), and the temperature of the ambient surface seawater derived from band 4 GOES 8 data was 22°C.

The heat balance equation is:

$$m_a C_a (T_a - 373) = m_w C_w (373 - 295) + m_w H_v \quad (1)$$

where C_a is the specific heat of andesite, 1200 J kg⁻¹ K⁻¹ (McBirney 1993); m_a is the mass of andesite, 1.0×10^{11} kg; T_a is the temperature of the Montserrat andesite = 850°C = 1123 K; C_w is the specific heat of water, 4128 J kg⁻¹ K⁻¹; H_v is the latent heat of vaporization, 2.5×10^6 J kg⁻¹. We can then solve for m_w , the water mass = 3.19×10^{10} kg.

This is a maximum mass of water, assuming all of the ash that reached the sea was used to evaporate the water with 100% efficiency. The efficiency of evaporation would be far less than 100% for several reasons. Larger fragments in the pyroclastic density current probably entered the sea, sank, and heated large quantities of water without reaching the boiling point, so that evaporation did not occur. It is likely that much of the heat exchange may have heated the water only slightly, not enough to boil. The VM cloud was estimated above to have a maximum mass of 1.5×10^8 kg (equivalent to 4.7×10^{14} J) of water vapour at 09:39 UT on 26 December 1997. This amounts to an efficiency of *c.* 5% if we assume that all of the H₂O in the cloud came from evaporation induced by the heat exchange between the pyroclastic density current and the sea. If the entire mass of andesitic ash (1.0×10^{11} kg) was fed into a buoyant 'thermal' plume model such as outlined by Sparks *et al.* (1997, fig. 7.23, p. 206), a cloud height of *c.* 15 km would result. If the entire steam mass estimated by the evaporation at 100% efficiency (3.19×10^{10} kg) was fed into a similar thermal model the height would be similar. This is close to the observed height of both the ash and VM clouds (15–17 km, see above). Exact agreement would be unlikely because the thermal energy of the andesite was partly transferred to seawater evaporation and part of the thermal energy was dissipated into heating of seawater without evaporation. It is likely that the rise of both the ash and VM cloud were nearly simultaneous and reinforced each other, so the height of both clouds is the result of their collective thermal energy.

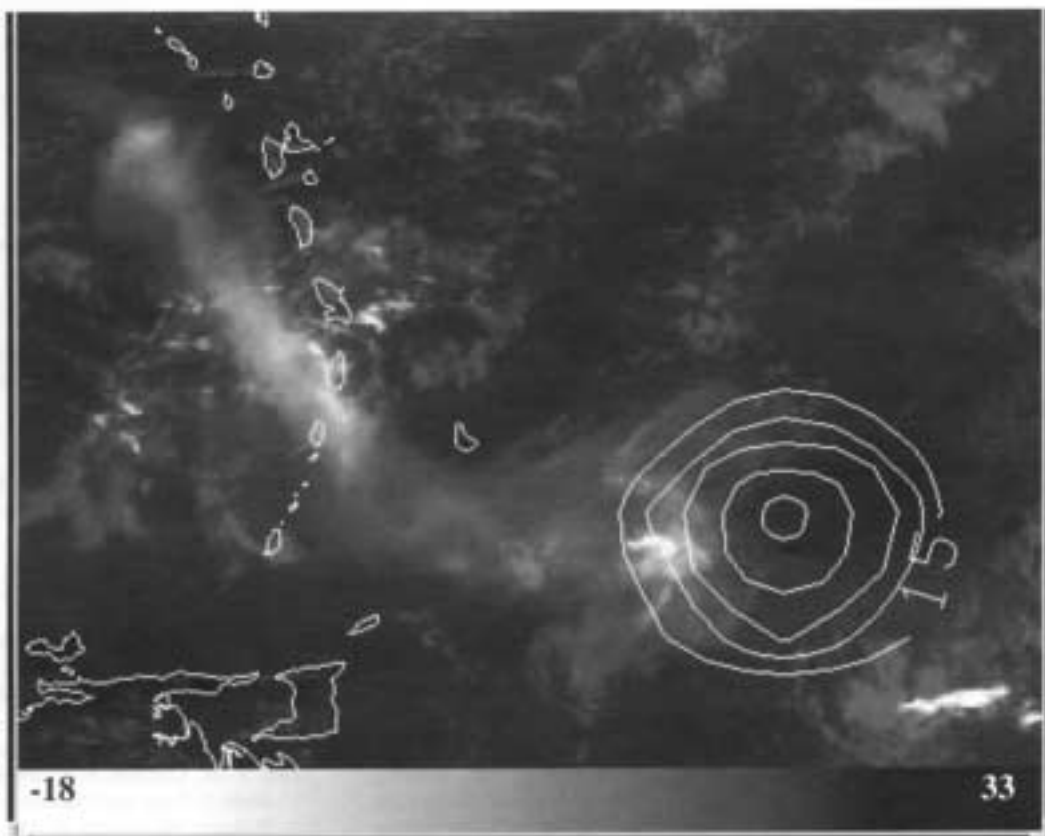
The effects of high humidity on volcanic cloud detection

Figure 2 shows the comparison of areas of the volcanic cloud using band 4 alone and the BTM method. The differences in area are largely due to the effects of high tropospheric humidity on a weak volcanic cloud signal. Coll & Caselles (1997) used real data to validate split-window algorithms for sea and land surface temperatures and showed that under humid conditions atmospheric transmission decreases with increased humidity. Rose & Prata (1997) found that high tropospheric water vapour in the tropics dramatically affected the BTM values by shifting volcanic cloud pixels with low optical depth to higher BTM values by up to about 3 K. This resulted in fewer pixels being identified as volcanic ash. Use of a variable BTM cutoff to distinguish the volcanic cloud is investigated by Yu (2000), who used a new method of discriminating the volcanic cloud, based on atmospheric corrections for both the band 4 and band 5 brightness temperatures and the BTM, which also shifts the retrieval grid significantly. These corrections allow more accurate estimates of ash masses and areas to be used in tropical regions where humidity is high. Based on Yu's (2000) preliminary work, the masses given in Table 2 are probably too low by factors of about three to five.

SO₂ and ash separation in the 26 December 1997 volcanic cloud

TOMS images at 15:43 UT of the positions of the SO₂ gas (Figs 9 and 17) and the volcanic ash (Fig. 10) show that the SO₂ was concentrated in the easternmost portion of the volcanic cloud. Since only one TOMS image was collected on 26 December 1997, it is not possible to determine if the SO₂ gradually separated from the volcanic cloud, or if it was leading the volcanic cloud to the east. The eastern edge of the SO₂ mass is not well known because it was at the edge of the TOMS swath. The SO₂ pattern seen by TOMS is circular and there was no tail of SO₂ into the volcanic cloud to the west, suggesting that the SO₂ was separated and was not interacting with the volcanic ash by 15:43 UT. Since the SO₂ and the highest portion of the volcanic cloud overlapped, it is most likely that the SO₂ rose to at least the maximum height reached by the ash (*c.* 15 km). It is clear that SO₂ did not rise above 17 km, which was the height of the tropopause, because the morphology of the plume does not reflect the effects of the change in wind direction and speed

Fig. 17. TOMS SO_2 burden contours at 15:43 UT (white lines showing contours every two Dobson Units from 15 to 23), superimposed over the GOES band 4 image (band 4 brightness temperatures in $^{\circ}\text{C}$) at 15:39 UT.



above 17 km. The wind changed speed and direction dramatically from 75 km h^{-1} to the SE at 17 km to 21 km h^{-1} to the SSW at 18 km. Table 3 lists volcanic clouds in which SO_2 separation from volcanic ash have been observed. Four explanations for the separation have been suggested, as listed below.

Gravitational sedimentation in the volcanic cloud. According to Holasek *et al.* (1996) SO_2 /ash separation may occur due to gravitational sedimentation of ash within the volcanic cloud. They performed experiments that illustrate the vertical segregation within a volcanic cloud where a relatively light, gas-rich portion of the volcanic cloud quickly rises, and the denser, ash-laden portion rises more slowly until neutral buoyancy is reached. In their study of the April 1982 eruption of El Chichón, Schneider *et al.* (1999) propose that gravitational separation is more likely to occur if the eruption intensity is high enough to emplace the volcanic cloud a few kilometres higher than the level of strong wind shear, where separation is aided by disparate wind directions; for example at the troposphere/stratosphere interface. While the volcanic clouds in Table 3 that experienced separation were emplaced several kilometres above the tropopause, the 26 December 1997 volcanic cloud was not. However, wind speeds were much slower at 10 km (72 km h^{-1}) than at 12 km (104 km h^{-1}) and 14 km (109 km h^{-1}), and the direction of the wind varied by only $c. 5^{\circ}$, so gravitational separation could have been accelerated by disparate wind speeds between 10 and 12 km altitude.

Table 3. Examples of gas/ash separation of volcanic clouds

Eruption (date)	SO_2 height (km)	Ash height (km)	Ref.
El Chichón (4/82)	22–26	19–21	Schneider <i>et al.</i> (1999)
Hudson (8/91)	14–18	10–14	Constantine <i>et al.</i> (1999)
Láscar (4/93)	>18	12–18	Shocker (1996)
Soufrière Hills (12/97)	14	4–12	Rose & Mayberry (2000)

Accelerated sedimentation caused by interaction between the VM and volcanic clouds. Separation of the SO_2 from ash in volcanic clouds may be promoted by the presence of hydrometeors (Herzog *et al.* 1998). According to Rose *et al.* (2000) the excess water from hydrometeors may interact with the ash in volcanic clouds, causing accelerated sedimentation of ash. Sedimentation in the 26 December 1997 volcanic cloud may have been accelerated by hydrometeors produced by interaction between the pyroclastic density current and seawater. The abundant accretionary lapilli from the eruption suggest that there was interaction between the ash in the volcanic cloud and the water in the VM cloud resulting in aggregation and accelerated sedimentation.

Formation of a gas-rich cap in the conduit. In this case, SO_2 /ash separation occurs before the volcano erupts, when a gas-rich cap forms in the magma conduit due to degassing of the magma body and movement of gas through a foamy, vesiculated magma body (Mader 1998). When an eruption occurs, the gas-rich cap is released first, rising higher than the ensuing volcanic cloud. We do not know whether any evidence for this idea exists, but it would require a gas-rich part of the explosion to have occurred in the first seconds of the event, perhaps many minutes before convection of the elutriated ash from the pyroclastic density current occurred.

Scavenging of SO_2 by hydrometeors in the VM cloud. Rose *et al.* (1995) propose that low SO_2 concentrations were observed in the Rabaul volcanic cloud because excess water in the cloud from hydrometeors scavenged or absorbed the SO_2 . They contend that scavenging occurred because the SO_2 in the volcanic cloud was either adsorbed on ice hydrometeors or was dissolved in the supercooled water in the volcanic cloud, which then formed ice around ash nuclei at $c. 6 \text{ km}$ altitude and fell out of the volcanic cloud. A similar process could have occurred in the 26 December 1997 volcanic cloud, but it is unclear why the highest part of the volcanic cloud would not have experienced it.

Conclusions

The abundance of satellite, meteorological and ground-based data available during the 26 December 1997 dome collapse and explosive decompression of Soufrière Hills Volcano provided an opportunity to analyse the dynamics of the volcanic and volcanogenic meteorological (VM) clouds produced, even though the early parts of the activity were in darkness.

The pyroclastic density current generated from the collapse of the lava dome produced a volcanic ash cloud. When it reached the sea, the hot ash heated the sea surface and evaporated seawater, producing a VM cloud. The volcanic cloud was recorded by the GOES 8, AVHRR and TOMS sensors; the more ephemeral VM cloud was recorded only by GOES 8 due to its greater frequency of data collection.

The volcanic cloud had a maximum mass of $c. 4.5 \times 10^7$ kg of fine (1–25 μm diameter) volcanic ash, and grew to a maximum area of about 100 000 km² at about 16:00 UT. Wind data were used to generate a trajectory model that helped define the three-dimensional geometry of the volcanic and VM clouds. The volcanic cloud rose to $c. 15$ km, growing in area to the SE while it simultaneously migrated SW, and the VM cloud was at similar altitudes but rose slightly higher to a maximum altitude of $c. 17$ km.

The VM cloud had a maximum mass of 1.5×10^8 kg of ice at 09:39 UT and grew in area for several hours. It interacted with the volcanic cloud, adding excess water/ice to it. The VM cloud masked the volcanic cloud from $c. 07:39$ to 13:39 UT by interfering with the signal of the silicate ash to the GOES 8 sensor, causing underestimations of ash mass values. The VM cloud dissipated after $c. 6$ hours, possibly due to evaporation or ice particles falling out of the cloud.

The higher spatial resolution of the AVHRR data showed a larger area of the fringe volcanic ash pixels than the GOES 8 data. The larger area of ash retrieved by the AVHRR sensor resulted in mean optical depth and total area values that were $c. 45\%$ higher, a total mass value that was 80% higher. These differences were higher than they would have been for larger eruptions. Even though the 26 December 1997 collapse was among the largest of the series of Soufrière Hills Volcano events of 1995–1999, it was one to three orders of magnitude smaller than eruptions of recent years elsewhere in the world.

The 26 December 1997 data set also provided an important example of a small volcanic cloud with complex evolution in a humid region. Applying the -0.5°C BTD cutoff to the volcanic cloud outlines only the densest 20% of the volcanic cloud. Atmospheric corrections must be made in order to detect the thin edges of small volcanic clouds in a humid atmosphere. The problem is more important when the eruption is very small, such as the 26 December 1997 event, so that the ash signal is nearly lost at the optically thin edges of the volcanic cloud.

TOMS data revealed that the SO₂ rose higher than the ash-rich portion of the 26 December 1997 volcanic cloud. The SO₂ may have been higher than the ash due to sedimentation causing accelerated fallout of the ash, and the shearing of the volcanic cloud by disparate wind speeds at different altitudes. Alternatively it could be the result of the early release of a gas-rich cap in the 26 December 1997 event or scavenging of the SO₂ by excess water in the ash cloud below 6 km altitude.

This project was funded by the NASA TOMS Research Program, the National Science Foundation, a Michigan Space Grant, and the American Geological Institute. We obtained the GOES data for this study through the co-operation of D. Johnson at the Research Applications Program at NCAR who received the data and allowed us to copy it from their data storage. M. Davies made the initial survey of all the 1997 Montserrat GOES data and got it ready to study. We would like to thank NASA Goddard Space Flight Center for the use of their facilities and their knowledge, and especially P. Newman, S. Schaefer, A. Krueger and N. Krotkov for sharing their expertise. D. Schneider and the staff of the Alaska Volcano Observatory helped to make the processing easier. Thanks also go to G. Norton, S. Young and the staff of the Montserrat Volcano Observatory for sharing information about the volcano. S. Sparks and the staff and students at the University of Bristol have also been instrumental to the success of this pro-

ject. M. Bursik, L. Glaze and D. Rothery made several helpful suggestions, and T. Druitt did an extraordinarily attentive editing job, which clarified much of the text.

References

- ALLEN, D. R., SCHOEBERL, M. R. & HERMAN, J. R. 1999. Trajectory modelling of aerosol clouds observed by TOMS. *Journal of Geophysical Research*, **104**, 27461–27471.
- BARCLAY, J., RUTHERFORD, M. J., CARROLL, M. R., MURPHY, M. D., DEVINE, J. D., GARDNER, J. & SPARKS, R. S. J. 1998. Experimental phase equilibria constraints on pre-eruptive storage conditions of the Soufrière Hills magma. *Geophysical Research Letters*, **25**, 3437–3440.
- BARRY, R. G. & CHORLEY, R. J. 1992. *Atmosphere, Weather and Climate*. Routledge, London.
- BAXTER, P. J., BONADONNA, C., DUPRE, R. ET AL. 1999. Cristobolite in volcanic ash of Soufrière Hills volcano, Montserrat, British West Indies. *Science*, **283**, 1142–1145.
- BONADONNA, C., MAYBERRY, G. C., CALDER, E. S. ET AL. 2002. Tephra fallout in the eruption of Soufrière Hills Volcano, Montserrat. In: DRUITT, T. H. & KOKELAAR, B. P. (eds) *The Eruption of Soufrière Hills Volcano, Montserrat, from 1995 to 1999*. Geological Society of London, Memoirs, **21**, 483–516.
- CAREY, S., SIGURDSSON, H., MANDEVILLE, C. & BRONTO, S. 1996. Pyroclastic flows and surges over water: An example from the 1883 Krakatau eruption. *Bulletin of Volcanology*, **57**, 493–511.
- COLL, P. D., CALDER, E. S., SPARKS, R. S. J. ET AL. 2002. Deposits from dome-collapse and fountain-collapse pyroclastic flows at Soufrière Hills Volcano, Montserrat. In: DRUITT, T. H. & KOKELAAR, B. P. (eds) *The Eruption of Soufrière Hills Volcano, Montserrat, from 1995 to 1999*. Geological Society of London, Memoirs, **21**, 231–262.
- COLL, C. & CASELLES, V. 1997. A split-window algorithm for land surface temperature from Advanced Very High Resolution Radiometer data: Validation and algorithm comparison. *Journal of Geophysical Research*, **102**, 16697–16713.
- CONSTANTINE, E. K., BLUTH, G. J. S. & ROSE, W. I. 2000. TOMS and AVHRR observations of drifting volcanic clouds from the August 1991 eruptions of Cerro Hudson. In: CRISP, J. & MOUGENIS-MARK, P. (eds) *Volcano Remote Sensing*, AGU Monograph, **116**, 45–64.
- DAVIES, M. A. & ROSE, W. I. 1998. GOES imagery fills gaps in Montserrat volcanic cloud observations. *Ess. Transactions American Geophysical Union*, **79**, 505–507.
- HERZOG, M., GRAF, H. F., TEXTOR, C. & OBERHUBER, J. M. 1998. The effect of phase changes of water on the development of volcanic plumes. *Journal of Volcanology and Geothermal Research*, **87**, 55–74.
- HOLASEK, R. E., WOODS, A. & SELF, S. 1996. Experiments on gas separation processes in volcanic umbrella clouds. *Journal of Volcanology and Geothermal Research*, **70**, 169–181.
- KIDDER, S. Q. & VONDER HAAR, T. H. 1995. *Satellite Meteorology*. Academic Press, San Diego.
- KROTKOV, N. A., TORRES, O., SEFTOR, C. ET AL. 1999. Comparison of TOMS and AVHRR volcanic ash retrievals from the August 1992 eruptions of Mount Spurr. *Geophysical Research Letters*, **26**, 455–458.
- KRUEGER, A. J. 1983. Sighting of El Chichon sulfur dioxide with the Nimbus 7 Total Ozone Mapping Spectrometer. *Science*, **220**, 1377–1378.
- KRUEGER, A. J., WALTER, L. S., BHARTIA, P. K., SCHNETZLER, C. C., KROTKOV, N. A., SPROD, I. & BLUTH, G. J. S. 1995. Volcanic sulfur dioxide measurements from the Total Ozone Mapping Spectrometer instruments. *Journal of Geophysical Research*, **100**, 14057–14076.
- LILLESAND, T. M. & KIEFER, R. W. 1987. *Remote Sensing and Image Interpretation*. John Wiley, New York.
- MADER, H. M. 1998. Conduit flow and fragmentation. In: GILBERT, J. S. & SPARKS, R. S. J. (eds) *The Physics of Explosive Volcanic Eruptions*. Geological Society, London, Special Publications, **151**, 815–823.
- MCCURNEY, A. R. 1993. *Igneous Petrology*. Jones and Bartlett, Boston.
- MCPETERS, R., BHARTIA, P. K., KRUEGER, A. ET AL. 1998. *Earth Probe Total Ozone Mapping Spectrometer (TOMS) data product user's guide*. NASA Reference Publication, **TP-1998-206895**.
- PULACK, J. B., TOON, O. B. & KHARE, B. N. 1973. Optical properties of some terrestrial rocks and glasses. *Icarus*, **19**, 372–389.
- PRATA, A. J. 1989. Infrared radiative transfer calculations for volcanic ash clouds. *Geophysical Research Letters*, **16**, 1293–1296.

- RITCHIE, L. J., COLE, P. D. & SPARKS, R. S. J. 2002. Sedimentology of deposits from the pyroclastic density current of 26 December 1997 at Soufrière Hills Volcano, Montserrat. *In*: DRUETT, T. H. & KOKELAAR, B. P. (eds) *The Eruption of Soufrière Hills Volcano, Montserrat, from 1995 to 1999*. Geological Society, London, Memoirs, **21**, 435–456.
- ROSE, W. I. & MAYBERRY, G. C. 2000. Use of GOES thermal infrared imagery for eruption scale measurements, Soufrière Hills, Montserrat. *Geophysical Research Letters*, **27**, 3097–3100.
- ROSE, W. I. & PRATA, A. J. 1997. Atmospheric corrections for two band infrared volcanic cloud discriminations and retrievals. *Eos, Transactions American Geophysical Union*, **F818**.
- ROSE, W. I. & SCHNEIDER, D. J. 1996. Satellite images offer aircraft protection from volcanic ash clouds. *Eos, Transactions American Geophysical Union*, **77**, 529–532.
- ROSE, W. I., DELENI, D. J., SCHNEIDER, D. J. *ET AL.* 1995. Ice in the 1994 Rabaul eruption cloud: Implications for volcanic hazard and atmospheric effects. *Nature*, **375**, 477–479.
- ROSE, W. I., BLUTH, G. J. S. & ERNST, G. G. J. 2000. Integrating retrievals of volcanic cloud characteristics from satellite remote sensors – a summary. *Philosophical Transactions of the Royal Society Series A*, **358**, 1585–1606.
- SCHNEIDER, D. J., ROSE, W. I., COLE, L. R., BLUTH, G. J. S., SPROD, I. E. & KRUEGER, A. J. 1999. Early evolution of a stratospheric volcanic eruption cloud as observed with TOMS and AVHRR. *Journal of Geophysical Research*, **104**, 4037–4050.
- SCHOEBERL, M. R., LAIT, L. R., NEWMAN, P. A. & ROSENFELD, R. E. 1992. The structure of the polar vortex. *Journal of Geophysical Research*, **97**, 7859–7882.
- SEFTOR, C. J., HSU, N. C., HERMAN, J. R. *ET AL.* 1998. Detection of volcanic ash clouds from Nimbus-7/TOMS. *Journal of Geophysical Research*, **102**, 16749–16760.
- SHANNON, J. M. 1996. *3-D reconstruction of the Mount Spurr volcanic clouds using AVHRR, TOMS, and wind trajectory data*. MS Thesis, Michigan Technological University.
- SHOCKER, H. L. 1996. *Lascar volcanic clouds of 1993: Merging of satellite-based remote sensing from TOMS, AVHRR and ATSR during three days of atmospheric residence*. MS Thesis, Michigan Technological University.
- SPARKS, R. S. J., BURSE, M. I., CAREY, S. W. *ET AL.* 1997. *Volcanic Plumes*. John Wiley & Sons, Chichester.
- SPARKS, R. S. J., BARCLAY, J., CALDER, E. S. *ET AL.* 2002. Generation of a debris avalanche and violent pyroclastic density current on 26 December (Boxing Day) 1997 at Soufrière Hills Volcano, Montserrat. *In*: DRUETT, T. H. & KOKELAAR, B. P. (eds) *The Eruption of Soufrière Hills Volcano, Montserrat, from 1995 to 1999*. Geological Society, London, Memoirs, **21**, 409–434.
- WEN, S. & ROSE, W. I. 1994. Retrieval of sizes and total masses of particles in volcanic clouds using AVHRR hands 4 and 5. *Journal of Geophysical Research*, **99**, 5421–5431.
- YU, T. 2000. *Improved algorithms for volcanic clouds using multispectral infrared remote sensing*. PhD Dissertation, Michigan Technological University.